Soil & Tillage Research 240 (2024) 106070

Contents lists available at ScienceDirect

Soil & Tillage Research

journal homepage: www.elsevier.com/locate/still

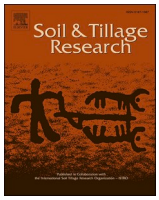

Modeling soil water and salt dynamics in cotton-sugarbeet intercropping and their monocultures with biochar application

Xiaofang Wang [a,b], Yi Li [a,b,*], Asim Biswas [c], Honghui Sang [d], Jianqiang He [a,b], De Li Liu [e], Qiang Yu [f], Hao Feng [f], Kadambot H.M. Siddique [g]

[a] Key Lab of Agricultural Soil and Water Engineering in Arid and Semiarid Areas/Ministry of Education, Yangling 712100, PR China
[b] College of Water Resources and Architectural Engineering/Northwest Agriculture and Forestry University, Yangling 712100, PR China
[c] School of Environmental Sciences, University of Guelph, Guelph, Ontario N1G 2W1, Canada
[d] School of Hydraulic and Ecological Engineering, Nanchang Institute of Technology, Nanchang 330099, PR China
[e] NSW Department of Primary Industries, Wagga Wagga Agricultural Institute, Wagga Wagga, NSW 2650, Australia
[f] State Key Laboratory of Soil Erosion and Dryland Farming on the Loess Plateau, Institute of Soil and Water Conservation, Northwest A&F University, Yangling, Shaanxi 712100, PR China
[g] The UWA Institute of Agriculture, and UWA School of Agriculture and Environment, The University of Western Australia, Perth, WA 6001, Australia

ARTICLE INFO

Keywords:
HYDRUS-2D
Numerical simulation
Root water uptake
Irrigation quota

ABSTRACT

Managing soil salinity in arid areas is a challenging task that is becoming increasingly difficult. Various management practices include using salt-tolerant crops like cotton and sugarbeet, plastic-mulched drip irrigation, intercropping, and biochar. However, studying the effectiveness of these practices can be difficult, costly, and time-consuming, as obtaining information on soil water and salt dynamics can be challenging. Numerical simulations show promise, but have limited application in simulating complex field experiments, such as adding ameliorants and intercropping systems. This study aimed to use a simulation model called HYDRUS-2D to simulate soil water and salt dynamics and root water uptake (RWU) in cotton and sugarbeet monocultures and intercropping with biochar application in an arid climate to minimize soil water losses through optimal irrigation under plastic-mulched drip irrigation systems. The results of a three-year field experiment were used to calibrate and validate the HYDRUS-2D model. The soil water and salt dynamics were measured in fields with biochar applied at three different rates [0 t ha^{-1} (CK), 10 t ha^{-1} (B10), and 25 t ha^{-1} (B25)]. The R^2, RRMSE and NSE showed that the soil hydraulic and solute transport parameters optimized in HYDRUS-2D satisfied simulation accuracy requirements. The simulation results showed that biochar application increased soil water and salt storage. Simulated RWU ranked as B10>B25>CK, consistent with soil water storage and yield. The B10 treatment showed promising application potential in RWU enhancement, evaporation and water drainage reduction, irrigation water conservation and farmers' income increment. This study provides a useful reference for agricultural production and social benefits in arid and semiarid areas.

1. Introduction

Two main challenges face sustainable agricultural ecosystem development: water resource scarcity and soil salinity (Meena et al., 2019). Water scarcity induces unhealthy and unfair water exploitation leading to degraded ecosystems and greater competition (Xie et al., 2022). The global area of saline-alkali soil is 935 million ha, 75% of which is in arid and semiarid areas in India, China, and Pakistan (Li et al., 2016). The salinized soil area is expanding by 1–2 million hectares per year, and expected to increase further in the coming decades due to intensified human activities and climate change (Hassani et al., 2021), causing annual global income losses of at least US$27.3 billion (Qadir et al., 2014). Improving salt-affected soils and developing water-saving agriculture are important strategies to ensure national food security and

Abbreviations: IWUE, irrigation water use efficiency; RWU, root water uptake; EC, electrical conductivity; θv, soil water content; SSC, soil salt content; DAS, days after sowing; LAI, leaf area index; R^2, coefficient of determination; RRMSE, relative root mean square error; SE, Nash-Sutcliffe efficiency coefficient; SWS, soil water storage; SSS, soil salt storage; Ea, soil evaporation; CRWU, cumulative RWU; CE, cumulative evaporation; CD, cumulative drainage.

* Corresponding author at: Key Lab of Agricultural Soil and Water Engineering in Arid and Semiarid Areas/Ministry of Education, Yangling 712100, PR China
E-mail address: liyi@nwafu.edu.cn (Y. Li).

https://doi.org/10.1016/j.still.2024.106070
Received 15 August 2023; Received in revised form 27 November 2023; Accepted 29 February 2024
Available online 6 March 2024

sustainable agricultural development (Srivastava et al., 2016).

In the arid to semiarid Xinjiang Uyghur Autonomous Region, the main cotton production area in China, about one-third of the arable land is threatened by salinization (Li et al., 2021), causing losses of about 720 million kg grain per year (about 8.6% of the total grain output) and 130.5 million kg cotton per year (about 9% of the total cotton output), equating to about 3.5 billion Yuan per year (8% of the total agricultural output value) (http://3w.detts.org/Item/7659.aspx). Due to its location, Xinjiang's food security depends on local crop production, contingent on irrigation and groundwater. Thus, it is critical to grow 'more crop per drop' by reducing water losses and improving irrigation water use efficiency (IWUE) to alleviate local agricultural development issues and meet food security (Ning et al., 2021). Various strategies have been proposed to address these challenges, such as plastic mulched drip irrigation (Ning et al., 2021), modifying farm management strategies, using soil amendments, and planting salt-tolerant crops like cotton (*Gossypium hirsutum* L.) and sugarbeet (*Beta vulgaris* L.) (Hong et al., 2017; Yang et al., 2016). Haas and Défago (2005) reported that monoculture systems, such as continuous cotton cultivation, decrease the quality and quantity of produce. In contrast, intercropping systems that cultivate two or more crops in the same field at the same time can increase land and water use efficiencies, reduce soil erosion, alleviate drought risk, and increase yield and farmer income (Gou et al., 2016; Ren et al., 2019; Zhang et al., 2018). However, few studies have investigated intercropping systems in arid and semiarid climates.

Biochar is a widely recommended soil amendment for improving soil quality in agricultural production systems (Zhao et al., 2020). Biochar is usually a stable carbon-rich porous material produced by pyrolysis of waste biomass materials (e.g. plant straw, cinder or wood chips) under oxygen-limited or oxygen-free conditions at temperatures ranging from 300 to 1000°C or hydrothermal carbonization at low temperature. The special characteristics of biochar affected the physical and chemical properties of the soil at some extent. The porous structure of biochar can reduce soil bulk density and increase soil porosity, which also induces biochar to effectively improve soil water capacity and retain more water (Abrol et al., 2016; Burrell et al., 2016). Biochar increases the organic carbon content of soil, which promotes the binding of polyvalent cations with soil particles, thereby improving the soil agglomeration stability and preventing soil degradation (Kim et al., 2016). Besides, biochar can also be employed as a source of nutrients including available nitrogen, available phosphorus and available potassium (Laghari et al., 2015; Zheng et al., 2021). The effect of biochar on soil nutrient retention and utilization was greater than that of direct nutrient supply (Qian et al., 2023). Owing to soil quality and nutrient condition, biochar has been regarded as an effective ameliorant in promoting plant growth and yield (Mehdizadeh et al., 2020; Zhao et al., 2020). However, the performance of biochar mainly depends on the source of raw material, pyrolysis parameters and an appropriate application amount (Fu et al., 2019; Saifullah et al., 2018), as excessive amounts can aggravate soil salinity in arid and semiarid climates with high ash contents (Liang et al., 2021) and question the economic feasibility of a production system.

Various management practices, including salt-tolerant crops under plastic mulched drip irrigation in an intercropping system supplied with biochar, have been adopted and tested in Xinjiang (Li et al., 2022b; Wang et al., 2022b). However, understanding the effects of these measures on soil water and solute transport, RWU, and soil water balance is critical for their success. Soil salinity and water scarcity complicate irrigation in Xinjiang. A high soil salt concentration reduces the amount of available water for RWU for plant function, crop production, and sustainable irrigation (Poulose et al., 2021). Soil evaporation and plant transpiration also play a vital role in the soil water balance, as do soil water and salt distribution and composition. However, monitoring these processes can be challenging, limiting our understanding of soil water and salt dynamics and RWU.

Numerical simulation is an efficient approach to investigating optimal irrigation management practices (Ahmad et al., 2018; Aggarwal et al., 2017), using models such as HYDRUS (1D/2D/3D) (Šimůnek et al., 1999) with its flexible application conditions including the following. (i) Development of reasonable irrigation schedules for salt management. Xu et al. (2019) used the HYDRUS-1D model to design an optimal soil desalting irrigation plan by simulating salt transport and the effects of different irrigation practices on soil desalting. Liu et al. (2021) determined the placement of the subsurface pipe below the clay layer to obtain the best water drainage and salt discharge effects using HYDRUS-2D simulation results for soil water and salt transport. (ii) Soil water movement under additive conditions. Wang et al. (2018a) first applied HYDRUS-1D to simulate soil water dynamics in homogeneous and layered water-repellent soils. They later simulated the RWU of summer maize grown in water-repellent soils and revealed the possible mechanisms of soil water repellency for decreasing yield (Wang et al., 2021a). Li et al. (2022a) recommended an optimal amount and mixed depth of biochar application according to simulation scenarios in HYDRUS-1D. (iii) Soil water and salt dynamics in intercropping systems. Li et al. (2015) simulated two-dimensional SWC distributions and designed an optimal irrigation plan for a tomato–corn intercropping system with HYDRUS-2D. Chen et al. (2022) used HYDRUS-2D to simulate soil nitrogen dynamics in a tomato–corn intercropping system with different crop spatial arrangements to determine the most suitable spatial arrangement. Overall, the HYDRUS model has been confirmed to simulate soil water and salt dynamics under different filed productivity improvement conditions, such as drip irrigation, biochar and intercropping. However, the performance of HYDRUS model for simulating soil water and salt dynamics under integrated application of plastic mulched drip irrigation, biochar-applied soils and intercropping systems need further study.

This study aimed to (1) calibrate and validate soil water hydraulic and solute transport parameters of biochar-applied soils; (2) simulate soil water and salt dynamics and RWU in cotton and sugarbeet monocultures and intercropping; (3) optimize irrigation schedules to reduce soil water losses under plastic mulched drip irrigation in Xinjiang.

2. Materials and methods

2.1. Experimental design

2.1.1. Study area and soil and biochar properties

The field experiments for monoculture and intercropping of cotton and sugarbeet with biochar applications were conducted at Bayingol Mongolian Autonomous Prefecture in the Xinjiang Uyghur Autonomous, China (86°56′ E, 40°53′ N) from 2018–2020. The area has a temperate continental desert climate, with an annual mean temperature of 10.9°C, precipitation of 34.1 mm, and pan evapotranspiration of 2417 mm.

Before crop sowing, soil samples were collected from the 0–100 cm soil layer. Soil particle composition was determined using a Malvern laser particle size analyzer. Soil textures were silty clay loam at 0–60 cm and sand at 60–100 cm depth (Wrb, 2006). Soil electrical conductivity (EC) was measured with a DDS-303 conductivity meter, with the average soil salt content (SSC) at 0–60 cm depth ranging from 0.1–0.2%, categorized as a light salinized level (Xu, 1980).

Biochar was prepared from the processing residue of palm (*Trachycarpus fortunei*) oil by slow pyrolysis at 600 ℃ under anaerobic conditions. The cooled biochar was milled to powdery consistency to increase contact with the soil, with a particle size <2 mm, bulk density of 0.5 g cm^{-3}, and specific surface area of 217 m^2 g^{-1}. The initial electrical conductivity ($EC_{1:5}$) of the biochar was 11.02 mS cm^{-1}. Ferrous sulfate was used to acidify biochar to a pH of less than 7 (eventually measured at 6.7) to prevent soil pH increasing in saline-alkaline soils following biochar application.

2.1.2. Field planting and irrigation systems

Three planting systems were used in the field experiments: cotton monoculture, cotton–sugarbeet intercropping, and sugarbeet

monoculture. Xinluzhong #66 and Detian #2 were the cotton (*Gossypium hirsutum* L.) and sugar beet (*Beta vulgaris* L.) varieties, respectively. The planting system for cotton monoculture comprised four rows of cotton plants, with one plastic film and two drip lines. The intercropping system comprised four rows of cotton intercropped with one row of sugarbeet. For sugarbeet monoculture, the planting system comprised thre rows of sugarbeet plants, with one plastic film and two drip lines. Figure S1 is a schematic diagram of the three planting patterns. The average discharge rate of each drip emitter was about 2.0 L h^{-1}.

2.1.3. Biochar, irrigation, and fertilizer applications

Before sowing, biochar was mixed into the top 0–30 cm soil layer. In 2018, the initial biochar application amounts were 0 t ha^{-1} (CK) and 10 t ha^{-1} (B10); in 2019 and 2020, 25 t ha^{-1} (B25) of biochar was added. Each treatment was replicated three times. Each plot had an area of 6 m×6 m, with the treatment plots in a randomized block design. The experiments were carried out between April 11 and September 24 in 2018 and 2019, and April 15 and September 20 in 2020.

The irrigation and fertilization application schedules were the same for all treatments each year. The irrigation quota was 260 mm for all three experimental years. For each crop growing season, 450, 265, and 100 kg ha^{-1} of urea (N≥46%), diammonium phosphate (P_2O_5≥46%), and potassium sulfate (K_2O≥52%), respectively, were applied as fertilizers. Table S1 presents the irrigation and fertilizer application schedules.

2.2. Data collection and processing

2.2.1. Meteorological and groundwater data

Meteorological data including rainfall, air temperature, relative humidity, solar radiation, and wind speed were collected using a portable small automatic weather station (HOBO U30, USA) installed at the experimental field. The average groundwater table in the study area ranged from 1.2–1.8 m. The daily groundwater table during crop growing periods was measured with a monitoring well.

ET_0 (mm) was estimated using the Penman-Monteith equation (Allen et al., 1998) (Figure S1).

2.2.2. Soil water content and soil salt content

Soil samples were collected with a steel auger on different days after sowing (DAS), every 10 cm within 0–40 cm and every 20 cm within 40–100 cm from 2018–2020. The oven drying method was used to obtain soil water content (θ_v). Soil samples were ground and passed through a 2 mm sieve. The soil salt content (SSC; g kg^{-1}) was calculated as SSC=3.4328$EC_{1:5}$+1.0513 (R^2=0.95) and converted to SSC_v as follows:

$$SSS_v = 1000 \times \frac{SSS \times BD}{\theta_V} \tag{1}$$

where SSC_v is the concentration in volume (mg cm^{-3}), and BD is the soil bulk density (g cm^{-3}).

2.2.3. Leaf area index and cotton and sugarbeet yields

Leaf area index (LAI) was measured using a tape, and calculated as the product of the greatest length and width (García-Vila et al., 2009):

$$LAI = 0.84 \times \varepsilon \sum_{i}^{m} \sum_{j}^{n} \frac{L_{ij} \times W_{ij}}{m \times 10^4} \tag{2}$$

where ε is actual cotton planting density (plant m^{-2}), m is the total number of measured plants, n is the total number of leaves on a single plant, L and W are leaf length and width (cm), respectively, I and j are the j^{th} leaf on the i^{th} plant, and 0.84 is the conversion coefficient (Zong et al., 2021).

Three strips (each 6.67 m^2) were randomly selected in each plot to measure yield. The number of cotton bolls with diameters >2 cm and the number of sugarbeet plants were recorded. Twenty cotton bolls were randomly selected from each of the lower third, middle third, and upper third of the cotton plants to calculate yield. The sugarbeet plants were dug up to weigh tubers and calculate yield.

The IWUE of the monocultures and intercropping system were calculated as follows:

$$IWUE = \begin{cases} \dfrac{Y_c}{IRR}, \text{cottonmonoculture} \\ \dfrac{P_c Y_c^{'} + P_s Y_s^{'}}{IRR}, \text{ int } ercropping \\ \dfrac{Y_s}{IRR}, \text{sugarbeetmonoculture} \end{cases} \tag{3}$$

where Y_c and Y_s are yields of cotton and sugarbeet in the monoculture system (t ha^{-1}), P_c and P_s are the planting proportion for cotton and sugarbeet in the intercropping system, $Y_c^{'}$ and $Y_s^{'}$ are the yields of cotton and sugarbeet (t ha^{-1}) in the intercropping system, respectively, and IRR is the irrigation amount (mm).

2.3. Numerical simulation of soil water and solute dynamics

2.3.1. Main theory

The Richards equation and convection-dispersion equation were used to describe soil water and solute transport dynamics:

$$\begin{cases} \dfrac{\partial \theta_v}{\partial t} = \dfrac{\partial}{\partial x}\left[K(\theta_v)\dfrac{\partial h}{\partial x}\right] + \dfrac{\partial}{\partial x}\left[K(\theta_v)\dfrac{\partial h}{\partial z}\right] + \dfrac{K(\theta_v)}{\partial z} - S(h) \\ \dfrac{\partial(\theta_c)}{\partial t} = \dfrac{\partial}{\partial x}\left(\theta_v D_x \dfrac{\partial C}{\partial x}\right) + \dfrac{\partial}{\partial z}\left(\theta_v D z \dfrac{\partial C}{\partial z}\right) - \dfrac{\partial(q_x C)}{\partial x} - \dfrac{\partial(q_z C)}{\partial z} \end{cases} \tag{4}$$

where θ_v is volumetric soil water content (cm^3 cm^{-3}), h is matric potential (cm), z is vertical soil depth (cm) (downward is positive), x is horizontal distance (cm), t is time (day), $K(\theta)$ is unsaturated soil water conductivity (cm day^{-1}), S(h) is root water uptake term (cm^3 cm^{-3} day^{-1}), C is solute concentration (mg cm^{-3}), D is saturated-unsaturated hydrodynamic dispersion coefficient (cm^2 day^{-1}), and q is water flux (cm day^{-1}). The diameter of the wetted surface area formed with drip irrigation was 10 cm. Water flux (q) was calculated as:

$$q = 1000 \frac{q^{'} t^{'}}{L^{'}} \tag{5}$$

where $q^{'}$ is emitter rate (L h^{-1}), $t^{'}$ is irrigation duration (h), and $L^{'}$ is wetted boundary width (cm).

The van Genuchten-Mualem equation (Van Genuchten, 1980) describes the soil water retention curve and soil hydraulic conductivity:

$$\theta(h) = \begin{cases} \theta_r + \dfrac{(\theta_s - \theta_r)}{(1 + |\alpha h|^n)^m}, h < 0 \\ \theta_s, h \geq 0 \end{cases} \tag{6}$$

$$K(h) = \begin{cases} K_s S_e^{l}\left[1 - \left(1 - S_e^{\frac{1}{m}}\right)^m\right]^2, h < 0 \\ K_s, h \geq 0 \end{cases} \tag{7}$$

where θ_s is saturated soil water content (cm^3 cm^{-3}), θ_r is residual water content (cm^3 cm^{-3}), K_s is saturated hydraulic conductivity (cm day^{-1}), saturation ratio $S_e = (\theta_s - \theta_r)/(\theta - \theta_r)$, l is pore-connectivity parameter (fixed at 0.5), α is inverse of the air-entry value, n (>1) is pore-size distribution index, and m=1–1/n.

A multiplication model was recommended to describe plant RWU under water and salinity stress conditions (Feddes et al., 1978):

$$S(h) = A(h) b(x, z, t) T_p L_p \tag{8}$$

where$A(h)$is a dimensionless stress response function, and L_p is the

length of the soil surface associated with transpiration (cm), L_p values of 50 cm, 50 cm, and 55 cm in cotton, sugarbeet, and cotton–sugarbeet intercropping were used, and $b(x, z, t)$ is the normalized root water uptake distribution function (cm^{-2}).

T_p is the potential transpiration rate (cm day^{-1}), estimated as:

$$T_p = ET_p - E_p \tag{9}$$

where ET_p is potential evaporation (cm day^{-1}), and $ET_p = K_c\, ET_0$, where K_c is crop coefficient.

K_c for the cotton–sugarbeet intercropping system was estimated using a comprehensive coefficient without considering the height difference between cotton and sugarbeet (Li et al., 2019):

$$K_c = \frac{P_c K_{cc} + P_s K_{cs}}{P_c + P_s} \tag{10}$$

where P_c and P_s are planting area proportions of cotton (=0.8) and sugarbeet (=0.2) in the intercropping system, and K_{cc} and K_{cs} are the crop coefficients of cotton and sugarbeet, respectively. Specific values for these parameters were adopted from the FAO Irrigation and Drainage Paper 56 (Allen et al., 1998).

E_p is estimated as (Belmans et al., 1983; Goudriaan, 1985):

$$Ep = ET_p\, e^{-k\,LAI} \tag{11}$$

where k is dimensionless plant canopy radiation attenuation coefficient ($0.35 < k < 0.75$), set at 0.55, 0.60, and 0.45 for cotton, sugarbeet, and cotton–sugarbeet intercropping, respectively (Aggarwal et al., 2017; Yang et al., 2019).

The HYDRUS-2D model was used to simulate soil water and solute dynamics.

2.3.2. Initial and boundary conditions

The model simulation area for soil water and solute dynamics was in a rectangular domain (120 cm × 68 cm). The simulation started 55, 55, and 50 DAS in 2018, 2019, and 2020, respectively, to improve the accuracy and decrease root effects during early growth. The observed θ_v and SSC_v were set as the initial conditions:

$$\begin{cases} \theta_v(x,z,t) = \theta_0(x,z), (-38 \le x \le 30, 0 \le z \le 120, t = 0) \\ c_v(x,z,t) = c_0(x,z), (-38 \le x \le 30, 0 \le z \le 120, t = 0) \end{cases} \tag{12}$$

where θ_0 and c_0 are the initial θ_v and initial salt content, respectively.

The upper boundary conditions are time-variable flux, no-flux, and atmospheric types for the dripper, mulched area, and no-mulched area, respectively. The lower boundary is the variable pressure head type to consider groundwater table depth changes. No-flux boundary conditions were set for the left and right boundaries (Fig. 1).

2.3.3. Model calibration, validation, and application

The CK treatment had two soil layers (0–60 cm, 60–120 cm), while the biochar-applied treatments had three soil layers (0–30 cm, 30–60 cm, and 60–120 cm). For initial soil hydraulic and salt transport parameters, please refer to Wang et al. (2022a) and Li et al. (2018). The parameters were calibrated by θ_v and SSC values of cotton monoculture treatments and validated by θ_v and SSC for the sugarbeet monoculture and cotton-sugarbeet intercropping treatments. The HYDRUS-2D model performance was evaluated using the coefficient of determination (R^2), relative root mean square error (RRMSE), and Nash-Sutcliffe efficiency coefficient (NSE).

After calibration and validation, the simulated θ_v and salt results were used to calculate RWU, evapotranspiration, soil water storage (SWS), soil salt storage (SSS), and soil water balance components from 0–40 cm depth. The optimized irrigation amounts in different years were obtained from soil water balance components at different crop growth stages. The distance in y direction (Δy) was set to 1 cm for ease of understanding. Thus, the digital SWS and SSS were obtained as follows:

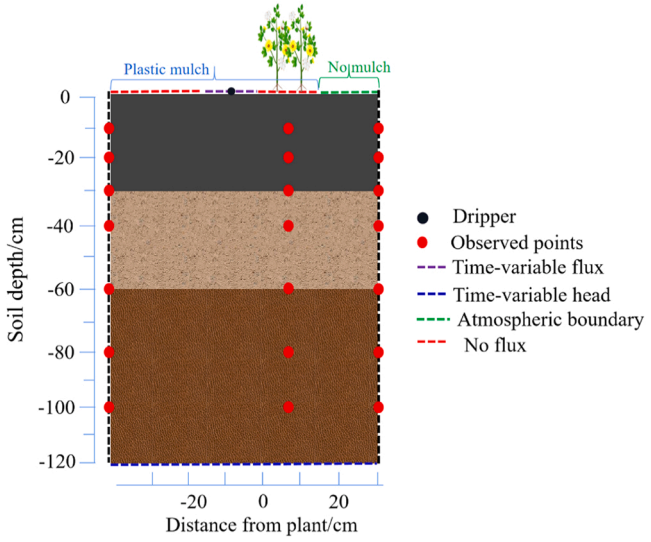

Fig. 1. Modeling domain, boundary condition setting, and observation points.

$$\begin{cases} SWS = \sum_{x=-38}^{30} \sum_{z=0}^{-40} \theta_v(x,z) \cdot \Delta y \\ SSS = \sum_{x=-38}^{30} \sum_{z=0}^{-40} C_v(x,z) \cdot \Delta y \end{cases} \tag{14}$$

3. Results

3.1. Crop growth parameters

The K_c values at seedling, squaring, flower-bolling, and boll-opening stages were 0.13, 0.69, 1.15, and 0.60 for cotton monoculture, 0.17, 1.16, 0.88, and 0.62 for cotton–sugarbeet intercropping, and 0.34, 0.80, 1.20, and 0.70 for sugarbeet monoculture, respectively. Biochar application affected the LAI and yields of cotton and sugarbeet in both monoculture and intercropping systems, and thus IWUE (Tables 1, 2, S2, and S3). The biochar-applied treatments had higher LAIs, crop yields, and IWUEs than the CK treatments (Table 3). The IWUE calculation for cotton and sugarbeet monocultures indicated the same change rates for yield and IWUE. The cotton monoculture yields and IWUE increased by 19.4% in 2018 (B10), 25.5% and 21.3% in 2019, and 45.5% and 18.2% in 2020 (B10 and B25, respectively) compared to CK. For cotton–sugarbeet intercropping, cotton yields increased by 16.5% in 2018 (B10), 22.5% and 25.0% in 2019, and 25.1% and 34.4% in 2020 (B10 and B25, respectively), and sugarbeet yields increased by 31.7% in 2018 (B10), 38.4% and 40.9% in 2019, and 79.4% and 24.3% in 2020 (B10

Table 1
Crop coefficient (K_c) and leaf area index (LAI) of cotton at different growth stages from 2018–2020. DAS is days after sowing. CK, B10, and B25 denote biochar rates of 0, 10, and 25 t ha^{-1}.

Treatment		Seedling stage (1–65 DAS)	Squaring stage (66–91 DAS)	Flow-bolling stage (92–136 DAS)	Boll-opening stage (137–163 DAS)
K_c		0.13	0.69	1.15	0.60
LAI	CK	0.16	1.38	4.39	3.56
2018	B10	0.32	1.81	5.94	4.72
LAI	CK	0.16	1.31	3.48	3.15
2019	B10	0.32	1.81	4.89	3.71
	B25	0.32	1.84	5.06	3.81
LAI	CK	0.16	0.80	3.53	3.11
2020	B10	0.16	2.49	4.33	3.86
	B25	0.16	2.21	3.67	3.23

Table 2
Crop yields and irrigation water use efficiency (IWUE) of three planting systems. CK, B10, and B25 denote biochar rates of 0, 10, and 25 t ha–1.

Year		Cotton		Intercropping system			Sugarbeet	
		Yield (kg ha^{-1})	IUWE (kg ha^{-1} mm^{-1})	Cotton yield (kg ha^{-1})	Sugarbeet yield (t ha^{-1})	IUWE (kg ha^{-1} mm^{-1})	Yield (t ha^{-1})	IUWE (t ha^{-1} mm^{-1})
2018	CK	5680	2.18	6314	20.8	3.55	82.3	0.32
	B10	6784	2.61	7358	27.4	4.37	106.6	0.41
2019	CK	5911	2.27	6040	19.8	3.38	71.1	0.27
	B10	7417	2.85	7398	27.4	4.38	99.3	0.38
	B25	7172	2.76	7547	27.9	4.47	88.4	0.34
2020	CK	4903	1.89	4773	18.9	2.92	92.1	0.35
	B10	7133	2.74	5969	33.9	4.45	123.0	0.62
	B25	5794	2.23	6417	23.5	3.89	113.7	0.44

Table 3
Soil hydraulic and solute transport parameters under different biochar treatments from 2018–2020. CK, B10, and B25 denote biochar rates of 0, 10, and 25 t ha–1.

Treatment	Soil depth (cm)		Soil hydraulic parameters					Solute transport parameters	
			θr (cm^3 cm^{-3})	θs (cm^3 cm^{-3})	α	n	Ks (cm day^{-1})	D_L (cm)	D_T (cm)
CK	0–60		0.08	0.38	0.08	1.8	25.0	30	3.0
	60–120		0.05	0.35	0.008	2.5	250	40	4.0
B10	2018	0–30	0.08	0.39	0.085	1.65	27.0	33	3.3
	2019		0.08	0.40	0.088	1.66	28.0	34	3.4
	2020		0.08	0.41	0.09	1.68	29.0	35	3.5
B25	2019	0–30	0.08	0.41	0.09	1.68	28.5	35	3.5
	2020		0.08	0.42	0.09	1.70	30.0	38	3.8

and B25, respectively). The intercropping IWUE increased by 23.1% in 2018 (B10), 29.6% and 32.2% in 2019, and 52.4% and 33.2% in 2020 (B10 and B25, respectively). The sugarbeet monoculture yields and IWUE increased by 29.5% in 2018 (B10), 39.7% and 24.3% in 2019, and 33.6% and 23.5% in 2020 (B10 and B25, respectively). The B10 treatment had the highest LAI, yield, and IWUE in all planting systems in all years except intercropping in 2019.

3.2. Modeling parameters and performance

We evaluated the effect of biochar application on the HYDRUS-2d simulation parameters (Table 3). Compared to the CK treatment, biochar application (B10 and B25) increased θ_s, K_s, and the soil's longitudinal dispersivity (D_L) and transverse dispersivity (D_T).

The simulation results of soil water and salt transport using the HYDRUS-2D model showed good agreement with the observed data (Figs. 2 and 3). The statistical analysis of the observed and simulated values revealed R^2 values > 0.75 and 0.83, RRMSE $< 9.4\%$ and 14.2%, and NSE > 0.73 and 0.80 for soil water and salt simulation, respectively. Therefore, the calibrated and validated soil hydraulic and solute transport parameters of the HYDRUS-2D model accurately captured the soil water and salt dynamics and thus could be used to analyze the soil water balance and predict irrigation scenarios.

3.3. Soil water and salt dynamics and storage

In cotton monoculture (Figure S3), the θ_v at 0–40 cm depth increased rapidly following irrigation and precipitation, gradually decreasing during the two consecutive irrigation events. Fig. 4 presents the two-dimensional soil water distribution at 0–40 cm depth before and after irrigation. Before irrigation, the root zone and no-mulch zone had very low θ_v. After irrigation, the soil water first infiltrated the zone around the dripper and then gradually increased θ_v in the no-mulched zone. The B10 and B25 treatments had higher θ_v than the CK treatment in all three planting systems.

The θ_v at 60–100 cm depth was less responsive to irrigation or precipitation. As soil depth increased, the θ_v increased the most within the 0–40 cm layer, followed by the 40–60 cm and 60–100 cm layers. Compared to CK with biochar-applied for the same experimental year, the θ_v in the same soil layer increased with increasing biochar application amount (Figure S3).

In line with θ_v dynamics, SWS at 0–40 cm depth also fluctuated with irrigation, increasing after irrigation and gradually decreasing thereafter until the next irrigation (Fig. 5). For example, in 2019, the SWS in the cotton monoculture, intercropping system, and sugarbeet monoculture ranged from 117–178, 109–166, and 116–168 cm^3 in the CK treatment, 120–186, 112–168, and 118–172 cm^3 in the B10 treatment, and 116–175, 114–177, and 122–179 cm^3 in the B25 treatment, respectively. Across all planting systems and experimental years, SWS was ranked B10>B25>CK. Overall, the intercropping system had lower SWS than the cotton monoculture.

Similar to soil water dynamics, irrigation and precipitation greatly affected soil salt dynamics at 0–10 cm, 10–20 cm, 20–30 cm, and 30–40 cm depth (Figure S4). However, in contrast to θ_v, soil salt decreased rapidly and then gradually increased during two consecutive irrigation events. Owing to the shallow and salty groundwater in the experimental site, soil salt content in topsoil fluctuated with seasons. Soil salt was migrated to the topsoil in the dry season, leached downward during irrigation and rainfall, and gradually accumulated in the topsoil again in late plant growth season when soil was dry. Following irrigation, salt in the surface layer was transported with infiltrated water, increasing the salt content in deeper layers. With increased irrigation time, salt at the surface increased due to soil evaporation. The SSC at 40–60 cm and 60–100 cm depth was less affected by irrigation. Biochar application increased SSC compared to CK, particularly in the B25 treatment in 2020 (Figure S4 h). This was mainly resulted from the rich plant ash content in biochar that caused the problem of introducing salt to soils when biochar was applied at a large dosage (B25 treatment). Figure S5 presents the two-dimensional soil salt distribution at 0–40 cm depth before and after irrigation. Before irrigation, soil water evaporation increased the surface salt content in the root zone and no-mulched zone. However, following irrigation, salt content in the root zone rapidly decreased, while it slightly decreased in the no-mulched zone.

Fig. 6 illustrates SSS at 0–40 cm depth for the cotton monoculture, cotton–sugarbeet intercropping, and sugarbeet monoculture. The SSS trends fluctuated with irrigation, gradually increasing by the end of the growing period. For instance, the SSS in the cotton monoculture, intercropping system, and sugarbeet monoculture in 2019 ranged 10–13, 7–13, and 10–14 g in the CK treatment, 11–14, 8–14, and 9–16 g in the B10 treatment, and 10–14, 11–15, and 12–16 g in the B25

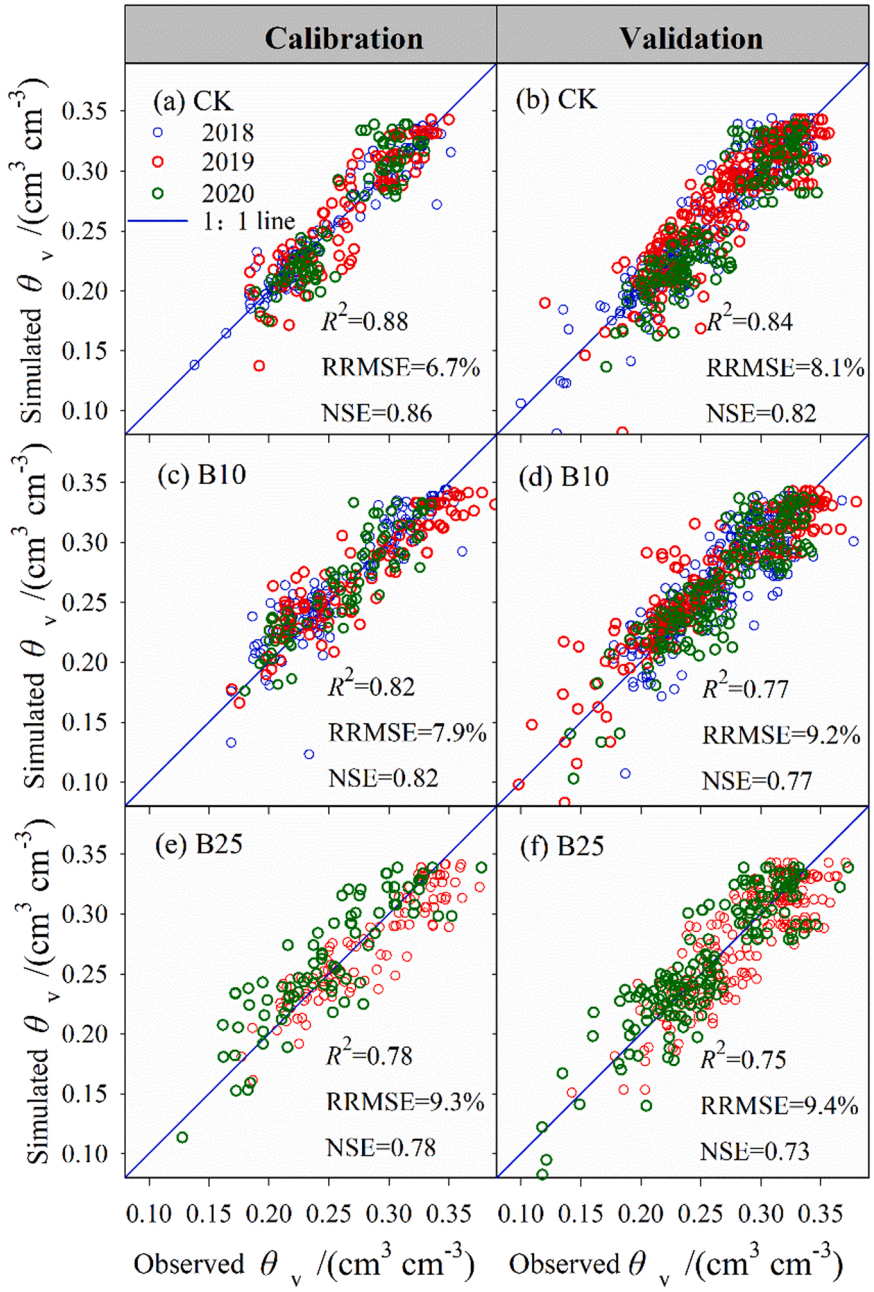

Fig. 2. Calibration and validation performance of the HYDRUS-2D for simulating soil water content (θ_v) under different biochar treatments. CK, B10, and B25 denote biochar rates of 0, 10 and 25 t ha^{-1}. R^2, RMSE, and NSE denote the coefficient of determination, relative root mean square error, and Nash-Sutcliffe efficiency coefficient, respectively.

treatment, respectively. Across all planting systems and experimental years, the SSS was ranked B25>B10>CK. The intercropping system generally had smaller SSS than the monocultures.

3.4. Soil water balance components

3.4.1. Root water uptake (RWU)

The biochar application amount and irrigation affected daily RWU. Figure S6 presents the two-dimensional distribution of daily RWU at 0–40 cm depth before irrigation (91 DAS) and after irrigation (93 DAS) in 2019. Irrigation greatly increased RWU, both horizontally and vertically. Compared to the CK treatment, the B10 and B25 treatments increased the RWU of cotton monoculture, cotton–sugarbeet intercropping, and sugarbeet monoculture before and after irrigation.

Fig. 7 shows the daily RWU fluctuation with irrigation. The largest daily RWU values for cotton monoculture were 0.69, 0.38, and 0.41 cm in the CK treatment and 0.79, 0.42, and 0.43 cm in the B10 treatment in 2018, 2019, and 2020, and 0.41 and 0.42 cm in the B25 treatment in 2019 and 2020, respectively (Fig. 7). The largest daily RWU values for the intercropping system were 0.88, 0.41, and 0.44 cm in the CK treatment and 1.55, 0.45, and 0.48 cm in the B10 treatment in 2018, 2019, and 2020, and 0.44 and 0.50 cm in the B25 treatment in 2019 and 2020, respectively. The largest daily RWU values for sugarbeet monoculture were 0.46, 0.34, and 0.43 cm in the CK treatment and 0.74, 0.46, and 0.45 cm in the B10 treatment in 2018, 2019, and 2020, and 0.41 and 0.44 cm in the B25 treatment in 2019 and 2020, respectively. Overall, the intercropping system had a larger RWU than cotton or sugarbeet monoculture (Fig. 7), and biochar application increased RWU compared to CK treatment. The RWU results were generally consistent with crop yield (Table 3), indicating that a higher RWU led to higher yield.

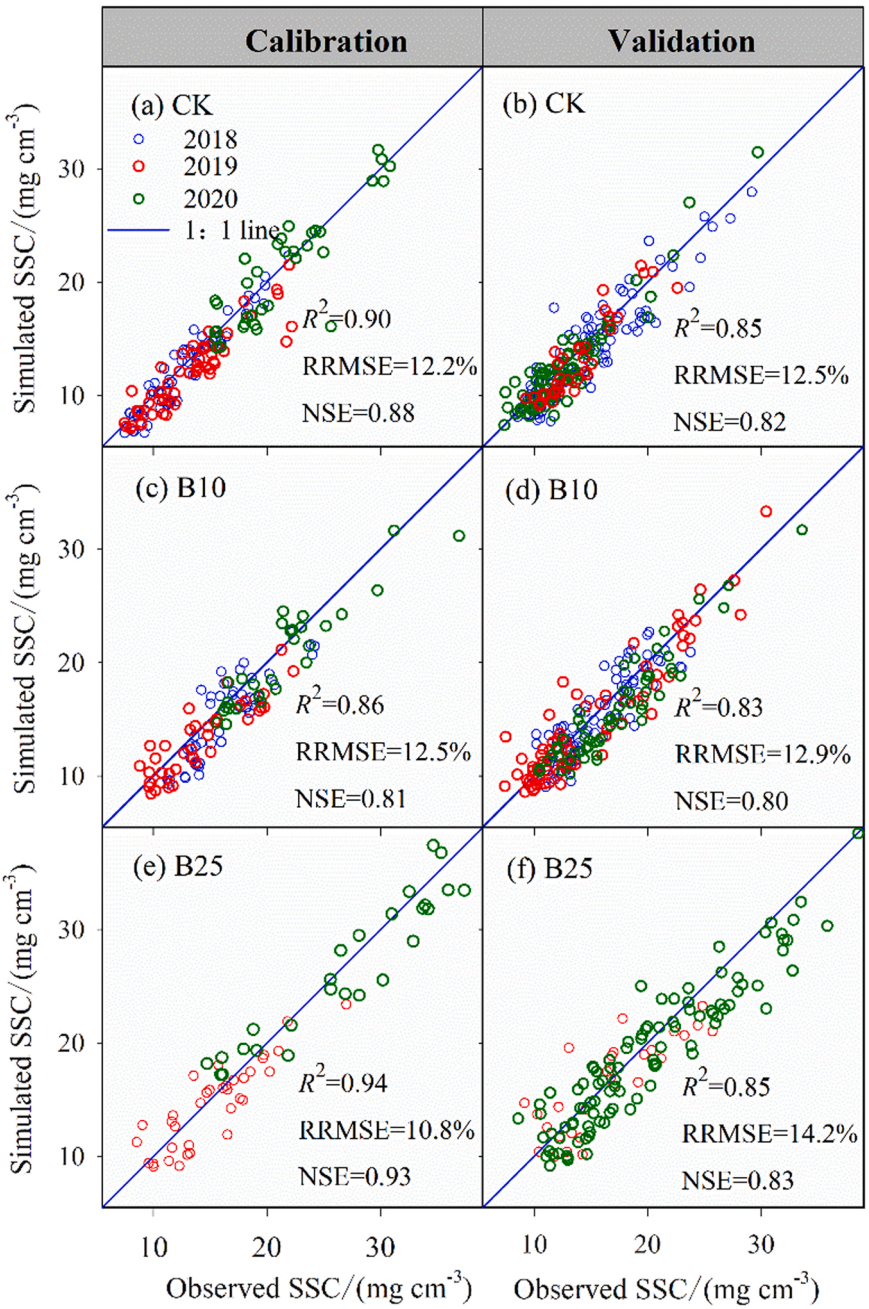

Fig. 3. Calibration and validation performance of the HYDRUS-2D model for simulating soil salt content (SSC) under different biochar treatments. CK, B10 and B25 denote biochar rates of 0, 10, and 25 t ha^{-1}. R^2, RMSE and NSE denote the coefficient of determination, relative root mean square error, and Nash-Sutcliffe efficiency coefficient, respectively.

3.4.2. *Soil evaporation (E_a)*

The largest daily E_a values for cotton monoculture were 0.08, 0.14, and 0.20 cm in the CK treatment and 0.07, 0.09, and 0.16 cm in the B10 treatment in 2018, 2019, and 2020, and 0.07 and 0.15 cm in the B25 treatment in 2019 and 2020, respectively (Fig. 8). The largest daily E_a for the intercropping system was 0.10, 0.13, and 0.16 cm in the CK treatment and 0.06, 0.05, and 0.15 cm in the B10 treatment in 2018, 2019, and 2020, and 0.06 and 0.13 cm in the B25 treatment in 2019 and 2020, respectively. The largest daily E_a for sugarbeet monoculture was 0.19, 0.15, and 0.16 cm in the CK treatment and 0.30, 0.12, and 0.15 cm in the B10 treatment in 2018, 2019, and 2020, and 0.13 and 0.14 cm in the B25 treatment in 2019 and 2020, respectively. The sugarbeet monoculture had a higher E_a than cotton monoculture and cotton–sugarbeet intercropping (Fig. 8). Biochar application decreased E_a, with the rates of change increasing with increase application amounts (Fig. 8).

3.4.3. *Soil water balance*

The soil water balance at 0–40 cm depth for cotton monoculture system indicated that biochar application increased the cumulative RWU (CRWU) more than the CK treatment but decreased cumulative evaporation (CE) except for the B25 treatment in 2020 (Table 5). The highest CRWU values in 2018, 2019, and 2020 were 24.2 cm (B10), 21.9 cm (B25), and 21.1 cm (B10), respectively. The highest CE values in 2018, 2019, and 2020 were 1.6 cm (CK), 5.2 cm (CK), and 3.7 cm (B25), respectively. The B10 treatment had the highest CRWU and lowest CE than the other treatments in the three experimental years. The cumulative drainage (CD) varied with biochar application amount and

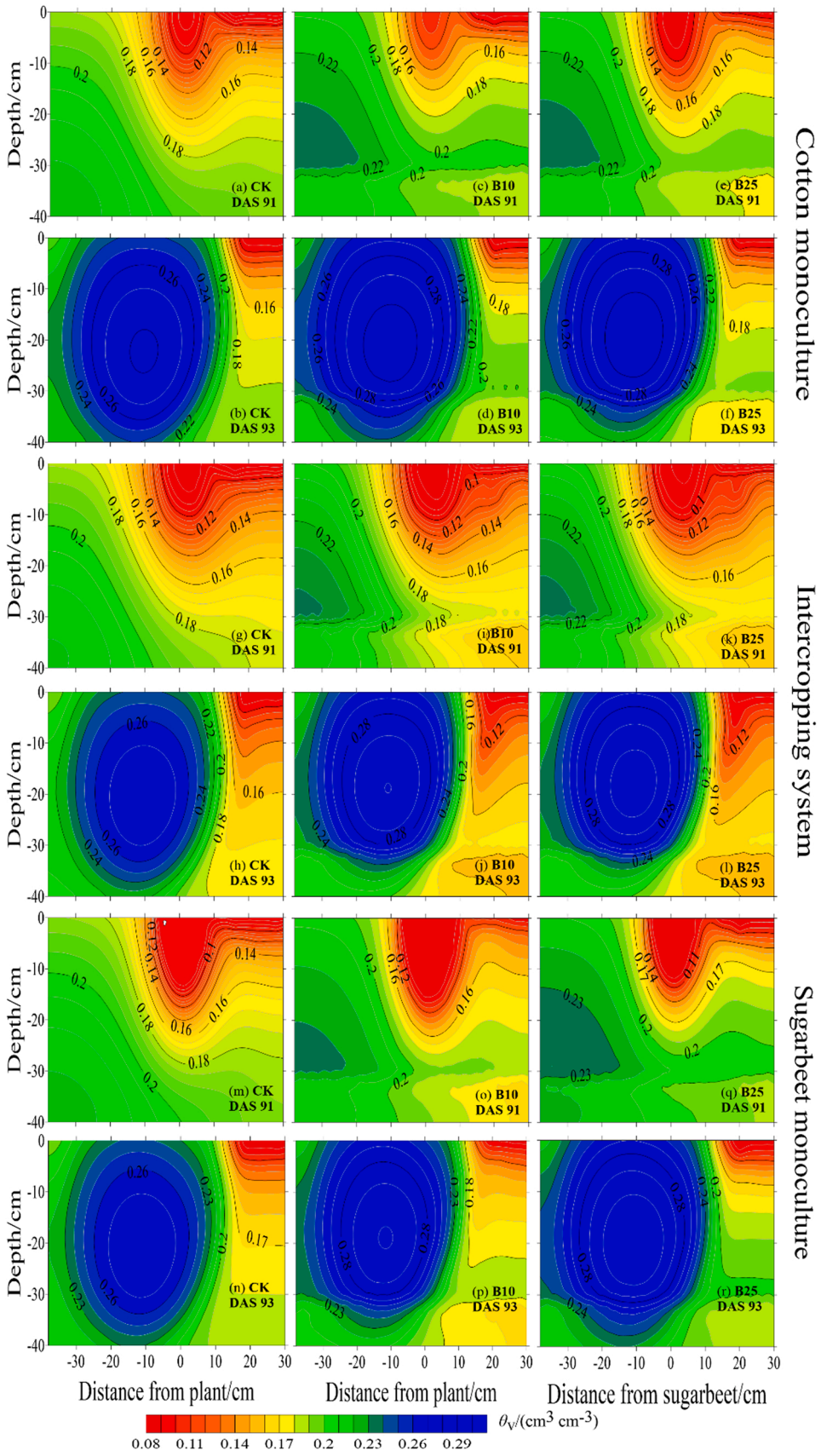

Fig. 4. Simulated soil water distribution from 0 to 40 cm soil depth at 91 DAS (1 day before irrigation) and 93 DAS (1 day after irrigation) under cotton and sugarbeet monoculture and intercropping. DAS is days after sowing. The contour line units are $cm^3\ cm^{-3}$. CK, B10, and B25 denote biochar rates of 0, 10, and 25 t ha^{-1}.

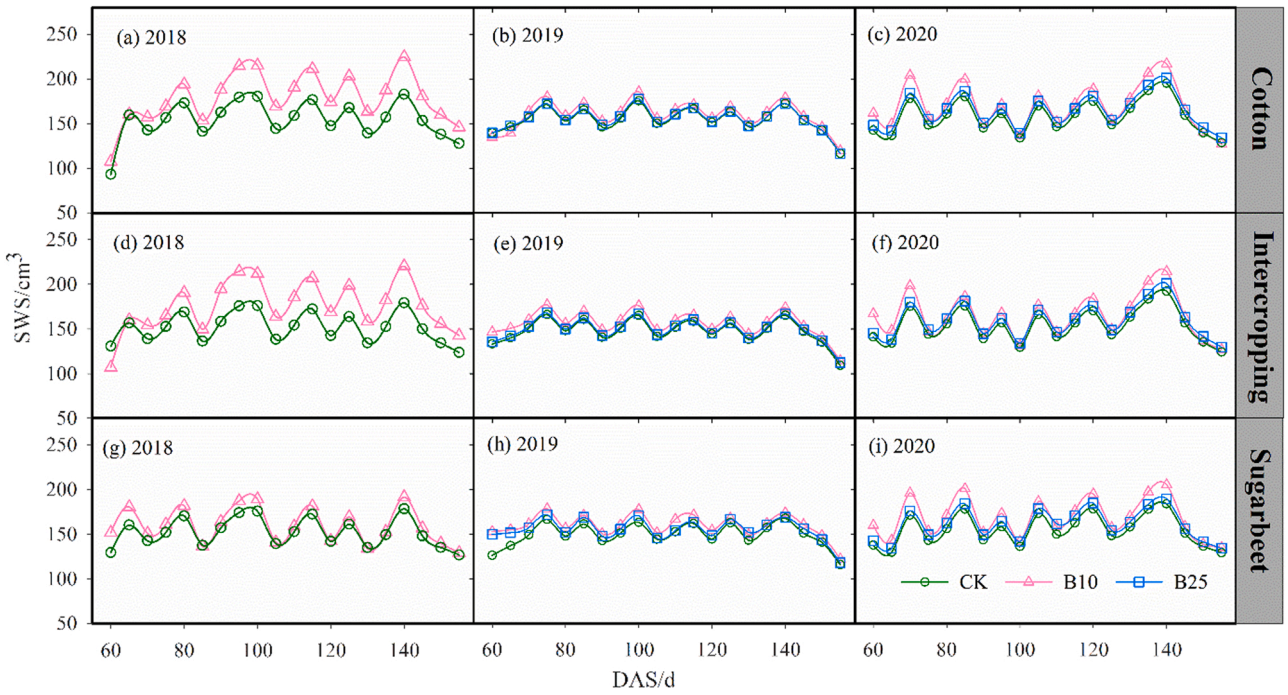

Fig. 5. Soil water storage (SWS) at 0–40 cm depth under different biochar treatments from 2018–2020. CK, B10, and B25 denote biochar rates of 0, 10, and 25 t ha^{-1}.

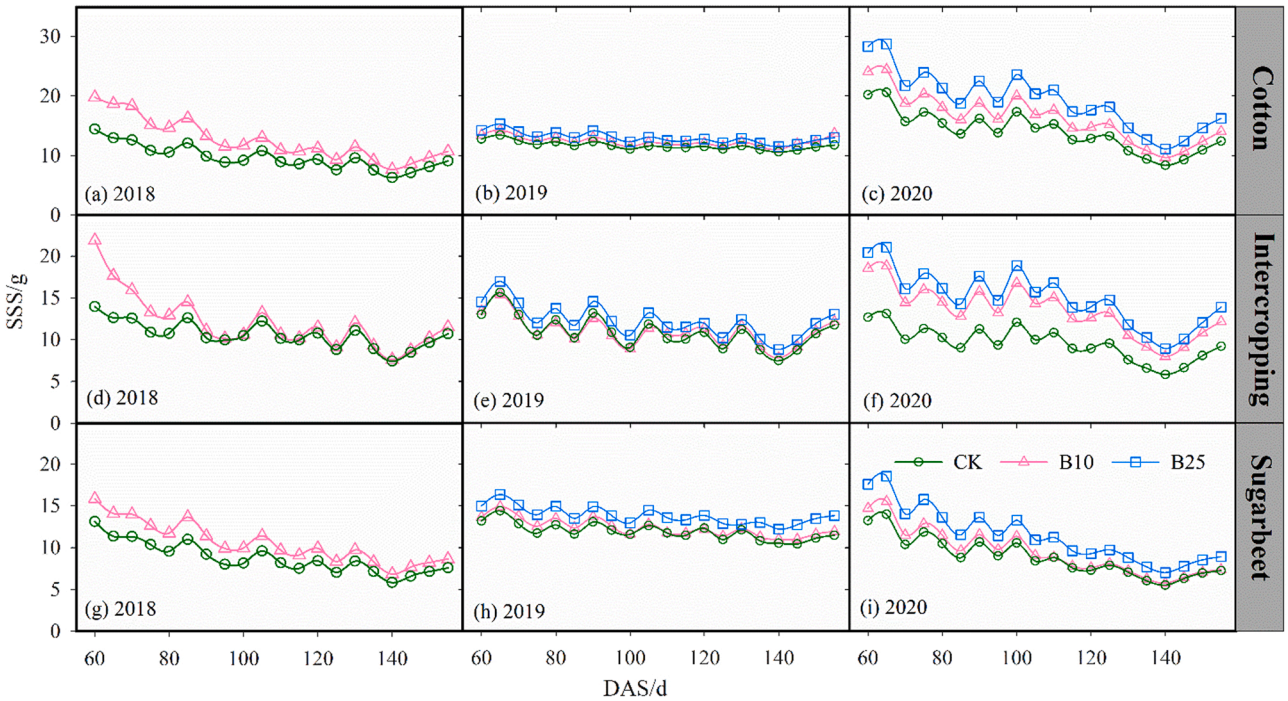

Fig. 6. Soil salt storage (SSS) at 0–40 cm depth under different biochar treatments from 2018–2020. CK, B10, and B25 denote biochar rates of 0, 10, and 25 t ha^{-1}.

experimental year. For the depth of the soil under study, positive CD values indicated that soil water drained into deeper soil layers, i.e. irrigation water may be wasted, while negative CD values indicated that soil water in the deeper soil layer was absorbed, i.e. salt in the deep soil would be absorbed by plants. Overall, excessive CD will result in a large amount of irrigation water waste, meanwhile, negative CD will threaten crop growth because of salt accumulation and water deficit. The B10 treatment had a larger CD than the CK treatment in 2018, with contrasting results in 2019 and 2020. The B10 and B25 treatments decreased CD by 44.6% and 43.1% in 2019 and 12.4% and 11.5% in 2020, respectively. Soil water balance results of intercropping and sugarbeet monoculture were similar to cotton monoculture (Tables S4 and S5).

3.5. *Application of HYDRUS-2D for optimizing irrigation schedule*

The optimized total irrigation amounts for the CK, B10, and B25 treatments were 220, 230, and 230 mm ha^{-1} in 2019 and 210, 220, and

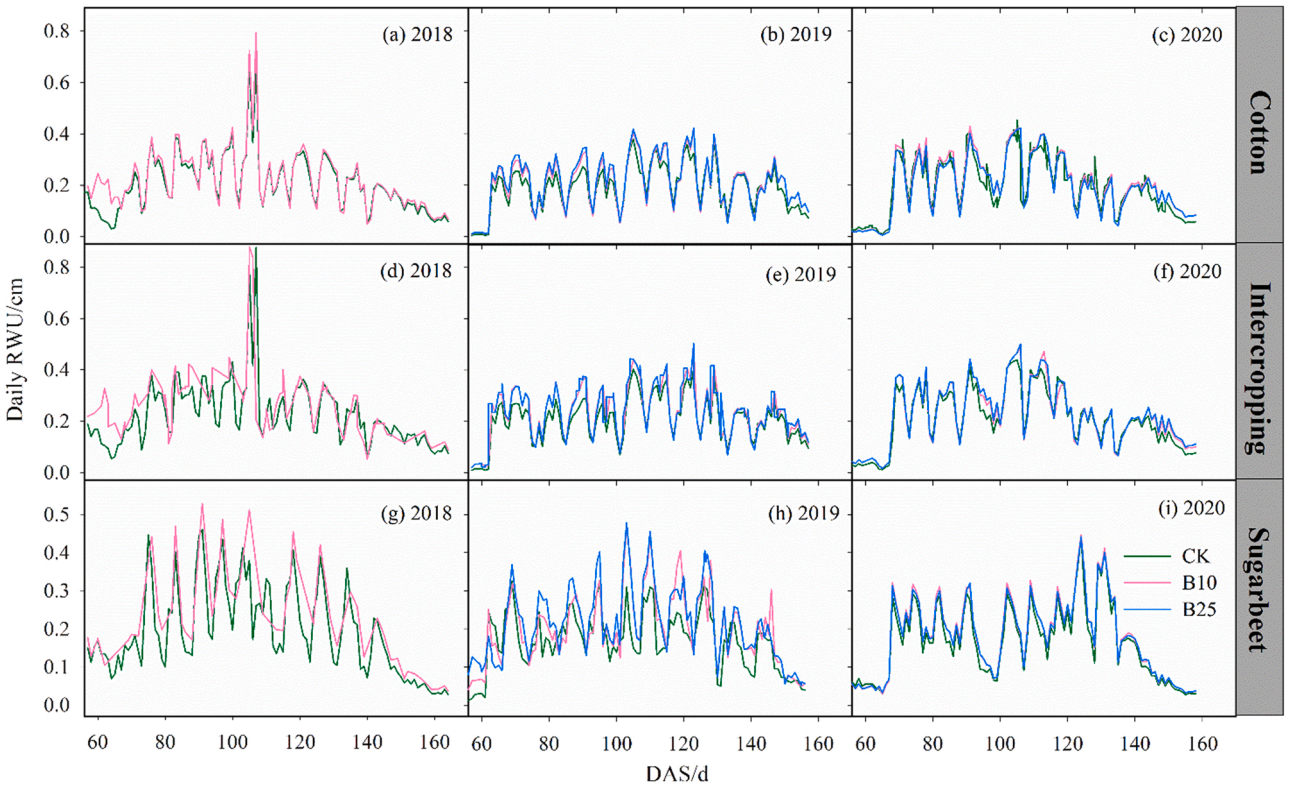

Fig. 7. Simulated average daily root water uptake (RWU) under different biochar treatments for cotton and sugarbeet monocultures and intercropping. CK, B10, and B25 denote biochar rates of 0, 10, and 25 t ha^{-1}.

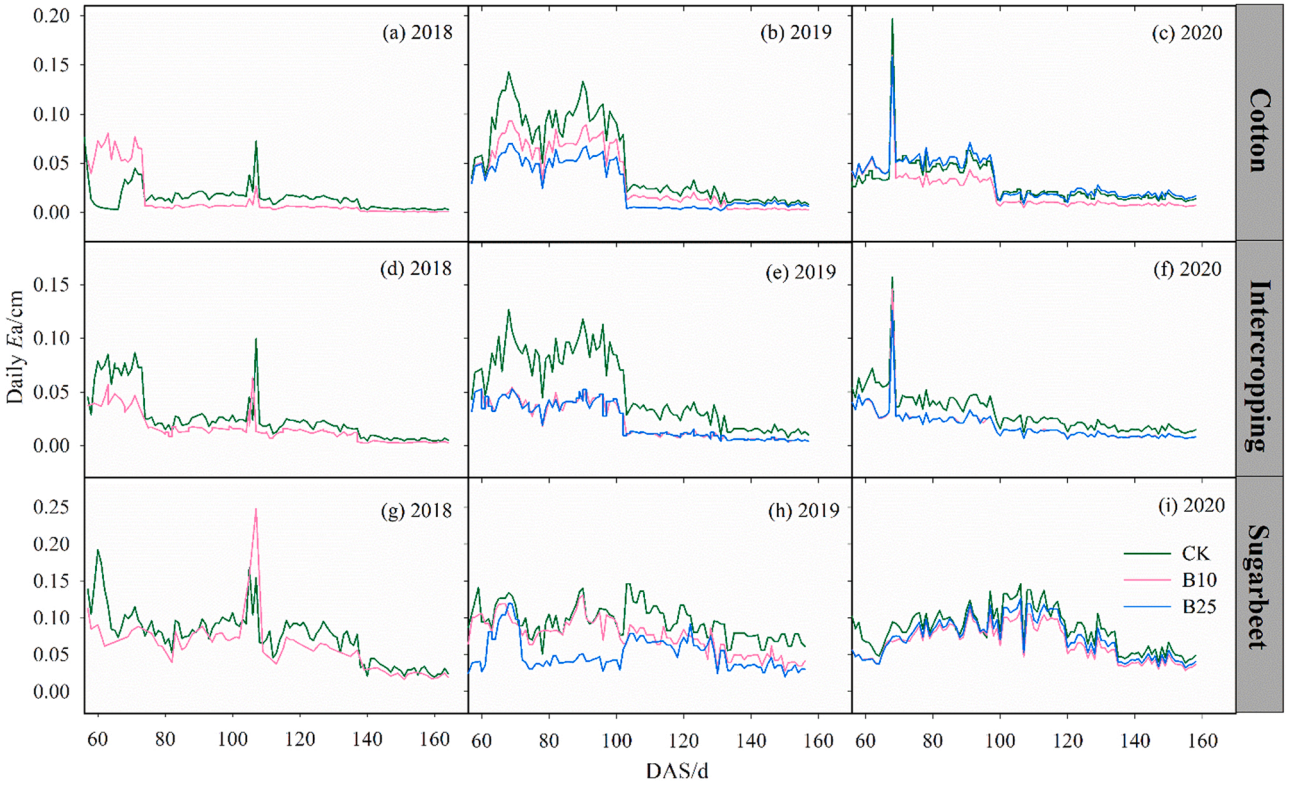

Fig. 8. Simulated average daily root water uptake (RWU) under different biochar treatments for cotton and sugarbeet monocultures and intercropping. CK, B10, and B25 denote biochar rates of 0, 10, and 25 t ha^{-1}.

220 mm ha^{-1} in 2020, respectively (Table 5), saving 40, 30, and 30 mm irrigation water in 2019 and 50, 40, and 40 mm irrigation water in 2020. The changes in irrigation amount in the CK, B10, and B25 treatments equated to 15.4%, 11.5%, and 11.5% in 2019 and 19.2%, 15.4%, and 15.4% in 2020, respectively. According to local irrigation water prices (0.15 Yuan m^{-3}), reducing irrigation water by 30 mm (300 m^3), 40 mm (400 m^3), and 50 mm (500 m^3) would save 45 Yuan (0.15 Yuan m^{-3} × 300 m^3), 60 Yuan (0.15 Yuan m^{-3} × 400 m^3) and 75 Yuan (0.15 Yuan m^{-3} × 500 m^3) per hectare. The soil water balance results showed that reducing irrigation amounts did not decrease the CRWU in the three treatments. The CD values in the CK, B10, and B25 treatments decreased from 6.5 to 0.0 cm, 2.8–0.2 cm, and 3.7–0.7 cm in 2019, and 7.8 to –0.1 cm, 7.3 to –0.1 cm, and 6.9 to –0.2 cm in 2020, respectively.

4. Discussion

4.1. Effects of integrating biochar and intercropping on soil water, salt, and crops

Both observed data and simulated results with HYDRUS-2D demonstrated the effects of integrating biochar and intercropping on soil water, salt, and crops. The mechanisms of biochar increasing the soil water is attributed to the vesicular structure, and high specific surface area (217 m2 g^{-1}) enhancing soil water retention capacity. In addition, soil physical properties were improved after the application of biochar (Wang et al., 2022b), which would enhance salt leaching. Biochar application increased LAI, crop yield, and IWUE, attributed to the biochar's abundant nutrient contents (e.g., N, P, and K) (Zhao et al., 2020). The biochar used in this study was confirmed to increase soil organic matter (Wang et al., 2022b), which caused a certain buffer effect, delayed the return of salt to soil, neutralized soil alkalinity, improved soil nutrients due to its high adsorption capacity (Zhao et al., 2020). Furthermore, Qian et al. (2023) revealed that the pyroligneous solution, which was a by-product of high-temperature pyrolysis to produce biochar, could further alleviate salinity pressure. However, the B25 treatment improved cotton and sugarbeet monoculture performance less than the B10 treatment (Tables 2 and 3). Similar results have been reported in other studies. For instance, Pandit et al. (2018) applied biochar at 0, 5, 10, 15, 25, and 40 t ha^{-1} to acidic silty loam soil grown with maize, reporting an optimal amount of 15 t ha^{-1} from an agronomic and economic perspective. Zhao et al. (2020) applied biochar at 0, 5, 10, 15, 20, 25, and 30 t ha^{-1} to maize, reporting 20 t ha^{-1} as the optimal amount based on soil properties and crop yield. This is mainly due to that biochar contains large amounts of ash, with many carbonates such as alkali and alkaline earth metals, heavy metals, and sesquioxides. When biochar is applied at a large dosage, it can increase SSC and threaten crop growth (Li et al., 2018). Thus, the biochar application increased the soil salt contents in all planting systems, as verified in the simulation results for salt dynamics (Figures S4 and S5).

LAI influenced Tp (Eq. 13), implying that biochar application and planting measures also affected Tp through affecting LAI. Accordingly, biochar application and intercropping affected the RWU (Table 4). Biochar increased the RWU compared to the CK treatment, likely due to the improved soil physical environment increasing LAI (Aggarwal et al., 2017). Cai et al. (2018) reported that silty soil had more water available for root extraction and, thus, RWU than stony soils. In this study, the biochar's abundant pores and low bulk density improved soil structure to some extent. The crop yield trend was consistent with RWU, i.e., a higher RWU led to a higher yield. Similarly, Aggarwal et al. (2017) reported that the treatment with the highest RWU had the greatest productivity. Wang et al. (2021) found that soil water repellency decreased the RWU of summer maize, further decreasing yield. They also reported that a higher RWU could reduce evaporation, as found in our study (Table 4).

Table 4
Simulated soil water balance components at 0–40 cm depth in different growing periods of cotton monoculture from 2018–2020. CRWU: cumulative root water uptake; CE: cumulative evaporation; IRR/PRE: irrigation/precipitation; CD: cumulative drainage.

Year	Treatment	DAS (d)	Initial SWC (cm)	Final SWC (cm)	CRWU (cm)	CE (cm)	IRR/PRE (cm)	CD (cm)
2018	CK	56–85	4.7	8.0	5.4	0.6	7.8	–1.5
		86–120	7.7	8.7	9.9	0.7	13.3	1.7
		121–164	8.2	6.0	7.3	0.4	6.2	0.7
		Total	20.6	22.7	22.6	1.6	27.3	1.0
	B10	56–85	9.1	9.0	6.5	1.1	7.8	0.3
		86–120	8.7	9.5	10.2	0.2	13.3	2.1
		121–164	9.1	6.7	7.6	0.1	6.2	0.8
		Total	26.9	25.3	24.2	1.5	27.3	3.2
2019	CK	56–85	9.1	9.1	4.2	2.6	7.8	1.2
		86–120	10.3	8.7	8.0	2.1	12.4	4.0
		121–157	8.1	6.3	7.0	0.6	7.2	1.4
		Total	27.6	24.0	19.3	5.2	27.4	6.5
	B10	56–85	9.1	11.2	5.3	1.8	7.8	–1.4
		86–120	10.5	9.7	9.2	1.5	12.4	2.7
		121–157	9.2	7.1	7.6	0.2	7.2	1.5
		Total	28.8	27.9	22.1	3.6	27.4	2.8
	B25	56–85	9.1	11.3	5.2	1.4	7.8	–1.0
		86–120	10.6	9.7	9.1	1.0	12.4	3.2
		121–157	9.2	7.1	7.6	0.3	7.2	1.5
		Total	28.9	28.1	21.9	2.7	27.4	3.7
2020	CK	50–85	8.8	7.8	5.3	1.6	7.0	1.1
		86–120	7.4	8.2	9.4	1.1	13.6	2.4
		121–158	7.9	6.0	5.5	0.6	8.4	4.3
		Total	24.2	22.0	20.2	3.3	29.0	7.8
	B10	50–85	9.1	8.8	5.1	1.5	7.0	0.7
		86–120	8.4	9.2	10.1	0.6	13.6	2.0
		121–158	9.0	6.6	5.9	0.3	8.4	4.5
		Total	26.4	24.6	21.1	2.5	29.0	7.3
	B25	50–85	9.1	8.9	4.7	1.9	7.0	0.6
		86–120	8.5	9.3	9.9	1.1	13.6	1.9
		121–158	9.0	6.6	5.7	0.7	8.4	4.4
		Total	26.7	24.8	20.3	3.7	29.0	6.9

4.2. Simulation of integration of mulched drip irrigation, biochar and intercropping

The HYDRUS model has been widely used due to its flexibility in boundary, initial, and experimental conditions (Yang et al., 2019; Zhang et al., 2022). However, when it was used to simulate soil water and salt dynamics with additive application, it was mostly focused on column infiltration or controlled experiments. Meanwhile, the simulations seldomly considered the integration of drip irrigation, additive application and intercropping in the field. For instance, Wang et al. (2017, 2018a, 2018b, 2021a, 2021b) conducted a series of studies using HYDRUS-1D to simulate water movement in additive applied soils, including column infiltration in homogeneous and heterogeneous water-repellent soils, and the RWU of summer maize in water-repellent soils under a rain shelter and its response to climate change. Wang et al. (2022) applied HYDRUS-2D to simulate the effects of biochar strategies, including application level, application depth, irrigation water depth, and initial soil moisture, on water loss and IWUE, revealing that biochar can slow soil water infiltration, reduce water loss, alleviate the waste of irrigation water, and increase IWUE. Li et al. (2022a) simulated soil water dynamics with HYDRUS-1D under different biochar application amounts and depths and recommended the optimal amount and depth of biochar application according to the simulation scenarios. Other studies used HYDRUS-2D to simulate soil water and solute dynamics and RWU in intercropping systems (Chen et al., 2022; Li et al., 2015). In this study, we enhanced the HYDRUS-2D model for simulating soil water and salt transport by considering the effects of biochar on the van Genuchten parameters and soil solute transport parameters under mulched and intercropping systems (Table 3). The biochar's low bulk density (0.5 g m^{-3}) and small particle size (<2 mm) increased θ_s and K_s. Moreover, the abundant, large pores in biochar increased soil pore size, further increasing K_s, D_L, and D_T (Wang et al., 2022b). After calibration and validation, the simulated soil water and salt content values generally agreed with the measured values. The HYDRUS-2D model also successfully captured the soil water and salt content dynamics following irrigation or precipitation. This study differs from other studies in that it is the first to use the HYDRUS-2D model to simulate soil water and salt dynamics and RWU in biochar-applied soils for cotton and sugarbeet monocultures and intercropping. Tables 5–7

Table 5
Adjusted irrigation schedules of cotton monocropping in 2019 and 2020 based on the soil water balance simulated by the HYDRUS-2D model.

Year	DAS (d)	Irrigation amount (mm)		
		CK	B10	B25
2019	65	22	22	22
	73	23	23	23
	82	25	25	25
	90	20	30	30
	98	20	20	20
	106	20	20	20
	114	20	20	20
	122	30	30	30
	129	20	20	20
	137	20	20	20
Total		220	230	230
2020	65	20	20	20
	71	20	20	20
	80	20	20	20
	91	25	30	30
	101	25	30	30
	108	25	30	30
	116	25	30	30
	123	20	20	20
	130	15	10	10
	135	15	10	10
Total		210	220	220

Table 6
Simulated soil water balance components at 0–40 cm depth in different growing periods of cotton monoculture in 2019 after adjusting irrigation. CRWU: cumulative root water uptake; CE: cumulative evaporation; IRR/PRE: irrigation/precipitation; CD: cumulative drainage.

Treatment	DAS (d)	Initial SWC (cm)	Final SWC (cm)	CRWU (cm)	CE (cm)	IRR/PRE (cm)	CD (cm)
CK	56–85	9.1	10.3	4.4	2.7	7.8	–0.4
	86–120	9.5	8.7	8.2	2.0	7.9	–1.4
	121–157	8.1	6.3	6.7	0.5	7.2	1.8
	Total	26.8	25.3	19.3	5.2	22.9	0.0
B10	56–85	9.1	11.2	5.1	1.8	7.8	–1.2
	86–120	8.9	7.9	9.4	1.4	10.9	1.1
	121–157	7.6	7.0	7.2	0.2	7.2	0.3
	Total	25.7	26.1	21.7	3.5	25.9	0.2
B25	56–85	9.1	11.3	5.2	1.4	7.8	–1.0
	86–120	8.3	7.7	9.3	0.9	10.9	1.3
	121–157	7.5	6.8	7.2	0.3	7.2	0.4
	Total	24.9	25.9	21.7	2.6	25.9	0.7

Table 7
Simulated soil water balance components at 0–40 cm depth in different growing periods of cotton monoculture in 2020 after adjusting irrigation. CRWU: cumulative root water uptake; CE: cumulative evaporation; IRR/PRE: irrigation/precipitation; CD: cumulative drainage.

Treatment	DAS (d)	Initial SWC (cm)	Final SWC (cm)	CRWU (cm)	CE (cm)	IRR/PRE (cm)	CD (cm)
CK	56–85	8.8	7.8	5.2	1.6	6.0	0.2
	86–120	7.4	8.2	9.4	1.1	10.0	–1.2
	121–157	7.9	6.0	5.4	0.6	5.0	0.9
	Total	24.2	22.0	20.0	3.3	21.0	–0.1
B10	56–85	8.9	8.8	5.1	1.5	6.0	–0.5
	86–120	8.4	9.2	10.2	0.6	12.0	0.3
	121–157	9.0	6.6	5.9	0.3	4.0	0.1
	Total	26.2	24.6	21.2	2.5	22.0	–0.1
B25	56–85	8.9	8.9	4.8	1.8	6.0	–0.6
	86–120	8.5	9.3	9.7	1.1	12.0	0.4
	121–157	9.0	6.6	5.7	0.7	4.0	–0.1
	Total	26.4	24.8	20.2	3.7	22.0	–0.2

4.3. Efficient utilization of agricultural resources

The integration of intercropping and biochar application in this study demonstrated an efficient utilization of agricultural resources, which increased water use efficiency and crop yields compared to monoculture crops with the same planting area, irrigation, and fertilizer amounts (Table 2). It was confirmed that integration of intercropping system with biochar application was an efficiency strategy to improve farmland productivity. Besides, this study furtherly conducted simulations with the HYDRUS-2D to optimize irrigation schedules, which was an important issue for alleviating water scarcity in the arid and semi-arid areas (Li et al., 2023). Previous studies have confirmed reliability of the HYDRUS-2D model in optimizing irrigation schedules. Zhang et al. (2022) applied HYDRUS-2D simulation results to optimize drip irrigation with alternate use of fresh and brackish waters in corn experiments under salt stress. Compared to conservation agriculture with flood irrigation and flood-irrigated puddled transplanted rice. Rana et al. (2022) used HYDRUS-2D model simulations to recommend conservation agriculture with subsurface drip irrigation for precise water utilization and reduced water loss. Groenveld et al. (2021) used the modified HYDRUS (2D/3D) model to determine the optimal irrigation water, NO_3^--N concentration, and seasonal NO_3^--N application for cucumber. Different from previous studies, this study used the HYDRUS-2D model to well simulate soil water and salt dynamics and calculated soil water balance, enabling the adjustment of irrigation schedules to save water resources under drip irrigation, biochar application and intercropping condition.

The CD results indicated that irrigation amounts were not always appropriate, with large amounts of wasted water induced by draining into the deeper soil layers rather than absorbed by plants. Therefore, the simulated CRWU with HYDRUS-2D after reducing irrigation water was not decreased, which was owing to reduction of CD and insurance of crop available water (3.5 part). It is important to verify the adjusted irrigation schedules with crop models to ensure they do not adversely impact crop yields. In addition, it should focus on real-time water dynamic simulation with the HYDRUS-2D model to provide a more powerful reference for optimizing irrigation schedules (i.e. when and how much water to irrigate) in the future study.

5. Conclusions

In this study, the integration strategy of mulched drip irrigation, biochar and intercropping was adopted to enhance agricultural water and soil resources use efficiency. Furthermore, the HYDRUS-2D model was applied to optimize irrigation schedule under biochar-applied and intercropping conditions, which was seldomly studied before. Results showed that biochar application and intercropping could effectively enhance crop yields and manage water and soil use. After the calibration and validation, the HYDRUS-2D model well-simulated soil water and salt dynamics of biochar-applied soils in both monoculture and intercropping systems. It revealed that biochar application increased SWS, reduced Ea and water drainage, and improved RWU, increasing crop yields. The optimal irrigation schedule was crucial to enhance IWUE, reduce production costs for farmers and raise the social economic benefits, especially for the arid and semi-arid areas. This study contributes to understanding biochar and intercropping mechanisms for the efficient utilization of agricultural resources and provides reference for managers to make decisions. In the future, it is important to verify the adjusted irrigation schedules with crop models. In addition, it also should focus on real-time water and salt dynamic simulation to provide a reference for optimizing irrigation schedules during the crop growth seasons to maintain agriculture sustainable development.

CRediT authorship contribution statement

Honghui Sang: Conceptualization, Data curation, Methodology, Software. **Asim Biswas:** Conceptualization, Resources, Supervision, Validation, Writing – review & editing. **De Li Liu:** Conceptualization, Methodology, Resources, Supervision, Writing – review & editing. **Jianqiang He:** Methodology, Software, Supervision, Writing – review & editing. **Qiang Yu:** Resources, Supervision, Writing – review & editing. **Kadambot H.M. Siddique:** Writing – review & editing. **Hao Feng:** Resources, Supervision. **Yi Li:** Conceptualization, Funding acquisition, Project administration, Resources, Supervision, Writing – review & editing. **Xiaofang Wang:** Conceptualization, Data curation, Formal analysis, Investigation, Methodology, Software, Validation, Writing – original draft, Writing – review & editing.

Declaration of Competing Interest

The authors declare that they have no known competing financial interests or personal relationships that could have appeared to influence the work reported in this paper.

Data availability

Data will be made available on request.

Acknowledgments

This research was jointly supported by the National Key Research and Development Program of China (No. 2022YFD1900401), the Key Research and Development Program of Xinjiang (No. 2022B02020–2), and the High-end Foreign Experts Introduction Project (G2022172025L).

Appendix A. Supporting information

Supplementary data associated with this article can be found in the online version at doi:10.1016/j.still.2024.106070.

References

Abrol, V., Ben-Hur, M., Verheijen, F.G.A., Keizer, J.J., Martins, M.A.S., Tenaw, H., Tchehansky, L., Graber, E.R., 2016. Biochar effects on soil water infiltration and erosion under seal formation conditions: rainfall simulation experiment. J. Soils Sediment. 16 (12), 2709–2719.

Aggarwal, P., Bh Abrol attacharyya, R., Mishra, A.K., Das, T.K., Šimůnek, J., Pramanik, P., Sudhishri, S., Vashisth, A., Krishnan, P., Chakraborty, D., Kamble, K. H., 2017. Modelling soil water balance and root water uptake in cotton grown under different soil conservation practices in the Indo-Gangetic Plain. Agriculture. Ecosyst. Environ. 240, 287–299.

Ahmad, M., Chakraborty, D., Aggarwal, P., Bhattacharyya, R., Singh, R., 2018. Modelling soil water dynamics and crop water use in a soybean-wheat rotation under chisel tillage in a sandy clay loam soil. Geoderma 327, 13–24.

Allen, R.G., Pereira, L.S., Raes, D., Smith, M., 1998. Crop Evapotranspiration-Guidelines for Computing Crop Water Requirements. Irrigation and Drainage Paper 56. FAO.

Belmans, C., Wesseling, J.G., Feddes, R.A., 1983. Simulation model of the water balance of a cropped soil: SWATRE. J. Hydrol. 63 (3), 271–286.

Burrell, L.D., Zehetner, F., Rampazzo, N., Wimmer, B., Soja, G., 2016. Long-term effects of biochar on soil physical properties. Geoderma 282, 96–102.

Cai, G., Vanderborght, J., Langensiepen, M., Schnepf, A., Hüging, H., Vereecken, H., 2018. Root growth, water uptake, and sap flow of winter wheat in response to different soil water conditions. Hydrol. Earth Syst. Sci. 22 (4), 2449–2470.

Chen, N., Li, X., Šimůnek, J., Shi, H., Zhang, Y., Hu, Q., 2022. Quantifying inter-species nitrogen competition in the tomato-corn intercropping system with different spatial arrangements. Agric. Syst. 201, 103461.

Fu, Q., Zhao, H., Li, T., Hou, R., Liu, D., Ji, Y., Zhou, Z., Yang, L., 2019. Effects of biochar addition on soil hydraulic properties before and after freezing-thawing. Catena 176, 112–124.

Gou, F., van Ittersum, M.K., Wang, G., van der Putten, P.E.L., van der Werf, W., 2016. Yield and yield components of wheat and maize in wheat–maize intercropping in the Netherlands. Eur. J. Agron. 76, 17–27.

Goudriaan, J., 1985. Crop Micrometeorology: a Simulation Study. Simulation Monographs, Pudoc, Wageningen, pp. 249.

Groenveld, T., Argaman, A., Šimůnek, J., Lazarovitch, N., 2021. Numerical modeling to optimize nitrogen fertigation with consideration of transient drought and nitrogen stress. Agric. Water Manag. 254, 106971.

Haas, D., Défago, G., 2005. Haas D, Defago G. Biological control of soil-borne pathogens by fluorescent pseudomonads. Nat. Rev. Microbiol. 3: 307-319. Nat. Rev. Microbiol. 3, 307–319.

Hassani, A., Azapagic, A., Shokri, N., 2021. Global predictions of primary soil salinization under changing climate in the 21st century. Nat. Commun. 12, 6663.

Hong, Y., Heerink, N., Jin, S., Berentsen, P., Zhang, L., van der Werf, W., 2017. Intercropping and agroforestry in China- Current state and trends. Agric., Ecosyst. Environ. 244, 52–61.

Laghari, M., Mirjat, M.S., Hu, Z., Fazal, S., Xiao, B., Hu, M., Chen, Z., Guo, D., 2015. Effects of biochar application rate on sandy desert soil properties and sorghum growth. Catena 135, 313–320.

Li, C., Xiong, Y., Qu, Z., Xu, X., Huang, Q., Huang, G., 2018. Impact of biochar addition on soil properties and water-fertilizer productivity of tomato in semi-arid region of Inner Mongolia, China. Geoderma 331, 100–108.

Li, P., Wu, J., Qian, H., 2016. Regulation of secondary soil salinization in semi-arid regions: a simulation research in the Nanshantaizi area along the silk road, Northwest China. Environ. Earth Sci. 75, 698.

Li, X., Shi, H., Šimůnek, J., Gong, X., Peng, Z., 2015. Modeling soil water dynamics in a drip-irrigated intercropping field under plastic mulch. Irrig. Sci. 33 (4), 289–302.

Li, X., Chen, N., Shi, H., Ding, Z., Peng, Z., 2019. Soil moisture distribution characteristics simulation of maize-tomato intercropping field with drip-irrigated under plastic mulch. Trans. Chin. Soc. Agric. Eng. 35 (10), 50–59.

Li, X., Zhang, J., Cai, X., Huo, Z., Zhang, C., 2023. Simulation-optimization based real-time irrigation scheduling: A human-machine interactive method enhanced by data assimilation. Agric. Water Manag. 276, 108059.

Li, Y., Ao, C., Zeng, W., Gaiser, Kumar, Srivastava, A., Wu, T., Huang, J, J., 2021. Simulating water and salt transport in subsurface pipe drainage systems with HYDRUS-2D. J. Hydrol. 592, 125823.

Li, Y., Liu, C., Liang, Z., Wang, X., Fan, X., Liu, D.L., Biswas, A., 2022a. Effect of biochar on soil properties and infiltration in a light salinized soil: Experiments and simulations. Eur. J. Soil Sci. 73 (4), 13279.

Li, Y., Yao, N., Liang, J., Wang, X., Jia, Y., Jiang, F., Liu, D.L., Hu, W., He, H., Javed, T., 2022b. Optimum biochar application rate for peak economic benefit of sugar beet in Xinjiang, China. Agric. Water Manag. 272, 107880.

Liang, J., Li, Y., Si, B., Wang, Y., Chen, X., Wang, X., Chen, H., Wang, H., Zhang, F., Bai, Y., Biswas, A., 2021. Optimizing biochar application to improve soil physical and hydraulic properties in saline-alkali soils. Sci. Total Environ. 771, 144802.

Meena, M.D., Yadav, R.K., Narjary, B., Yadav, G., Jat, H.S., Sheoran, P., Meena, M.K., Antil, R.S., Meena, B.L., Singh, H.V., Singh Meena, V., Rai, P.K., Ghosh, A., Moharana, P.C., 2019. Municipal solid waste (MSW): Strategies to improve salt affected soil sustainability: A review. Waste Manag. 84, 38–53.

Mehdizadeh, L., Moghaddam, M., Lakzian, A., 2020. Amelioration of soil properties, growth and leaf mineral elements of summer savory under salt stress and biochar application in alkaline soil. Sci. Hortic. 267, 109319.

Ning, S., Zhou, B., Shi, J., Wang, Q., 2021. Soil water/salt balance and water productivity of typical irrigation schedules for cotton under film mulched drip irrigation in northern Xinjiang. Agric. Water Manag. 245, 106651.

Pandit, N.R., Mulder, J., Hale, S.E., Zimmerman, A.R., Pandit, B.H., Cornelissen, G., 2018. Multi-year double cropping biochar field trials in Nepal: Finding the optimal biochar dose through agronomic trials and cost-benefit analysis. Sci. Total Environ. 637-638, 1333–1341.

Poulose, T., Kumar, S., Ganjegunte, G.K., 2021. Robust crop water simulation using system dynamic approach for participatory modeling. Environ. Model. Softw. 135, 104899.

Qadir, M., Quillérou, E., Nangia, V., Murtaza, G., Singh, M., Thomas, R.J., Drechsel, P., Noble, A.D., 2014. Economics of salt-induced land degradation and restoration. Nat. Resour. Forum 38, 282–295.

Qian, S., Zhou, X., Fu, Y., Song, B., Yan, H., Chen, Z., Sun, Q., Ye, H., Qin, L., Lai, C., 2023. Biochar-compost as a new option for soil improvement: Application in various problem soils. Sci. Total Environ. 870, 162024.

Rana, B., Parihar, C.M., Nayak, H.S., Patra, K., Singh, V.K., Singh, D.K., Pandey, R., Abdallah, A., Gupta, N., Sidhu, H.S., Gerard, B., Jat, M.L., 2022. Water budgeting in conservation agriculture-based sub-surface drip irrigation using HYDRUS-2D in rice under annual rotation with wheat in Western Indo-Gangetic Plains. Field Crops Res. 282, 108519.

Ren, J., Zhang, L., Duan, Y., Zhang, J., Evers, J.B., Zhang, Y., Su, Z., van der Werf, W., 2019. Intercropping potato (Solanum tuberosum L.) with hairy vetch (Vicia villosa) increases water use efficiency in dry conditions. Field Crops Res. 240, 168–176.

Saifullah, Dahlawi, S., Naeem, A., Rengel, Z., Naidu, R., 2018. Biochar application for the remediation of salt-affected soils: Challenges and opportunities. Sci. Total Environ. 625, 320–335.

Šimůnek, J., Šejna, M., van Genuchten, M.T., 1999. The HYDRUS-2D Software Package for Simulating the Two-dimensional Movement of Water, Heat, and Multiple Solutes in Variably-saturated Media. Version 2.0.

Van Genuchten, T.M., 1980. A Closed-form Equation for Predicting the Hydraulic Conductivity of Unsaturated Soils1. Soil Sci. Soc. Am. J. 44 (5), 892.

Wang, H., Shao, D., Ji, B., Gu, W., Yao, M., 2022a. Biochar effects on soil properties, water movement and irrigation water use efficiency of cultivated land in Qinghai-Tibet Plateau. Sci. Total Environ. 829, 154520.

Wang, X., Li, Y., Si, B., Ren, X., Chen, J., 2018a. Simulation of Water Movement in Layered Water-Repellent Soils using HYDRUS-1D. Soil Sci. Soc. Am. J. 82 (5), 1101–1112.

Wang, X., Li, Y., Wang, Y., Liu, C., 2018b. Performance of HYDRUS-1D for simulating water movement in water-repellent soils. Can. J. Soil Sci. 98 (3), 407–420.

Wang, X., Li, Y., Chau, H.W., Tang, D., Chen, J., Bayad, M., 2021a. Reduced root water uptake of summer maize grown in water-repellent soils simulated by HYDRUS-1D. Soil Tillage Res. 209, 104925.

Wang, X., Li, Y., Chen, X., Wang, H., Li, L., Yao, N., Liu, D.L., Biswas, A., Sun, S., 2021b. Projection of the climate change effects on soil water dynamics of summer maize grown in water repellent soils using APSIM and HYDRUS-1D models. Comput. Electron. Agric. 185, 106142.

Wang, X., Li, Y., Wang, H., Wang, Y., Biswas, A., Wai Chau, H., Liang, J., Zhang, F., Bai, Y., Wu, S., Chen, J., Liu, H., Yang, G., Pulatov, A., 2022b. Targeted biochar application alters physical, chemical, hydrological and thermal properties of salt-affected soils under cotton-sugarbeet intercropping. Catena 216, 106414.

Wrb, I., 2006. World Reference Base for Soil Resources (2nd ed.).

Xie, J., You, J., Ma, Z., Deng, X., Lin, P., Gao, J., 2022. Methodology for including reservoir regulation in water scarcity evaluation. J. Clean. Prod. 365, 132657.

Xu, C., Tian, J., Wang, G., Nie, J., Zhang, H., 2019. Dynamic Simulation of Soil Salt Transport in Arid Irrigation Areas under the HYDRUS-2D-Based Rotation Irrigation Mode. Water Resour. Manag. 33 (10), 3499–3512.

Xu, Z., 1980. The Improvement of Saline-alkali Soil in Xinjiang. Volksverlag Xinjiang, Xinjiang.

Yang, P., Hu, H., Tian, F., Zhang, Z., Dai, C., 2016. Crop coefficient for cotton under plastic mulch and drip irrigation based on eddy covariance observation in an arid area of northwestern China. Agric. Water Manag. 171, 21–30.

Yang, T., Šimůnek, J., Mo, M., McCullough-Sanden, B., Shahrokhnia, H., Cherchian, S., Wu, L., 2019. Assessing salinity leaching efficiency in three soils by the HYDRUS-1D and -2D simulations. Soil Tillage Res. 194, 104342.

Zhang, D., Du, G., Sun, Z., Bai, W., Wang, Q., Feng, L., Zheng, J., Zhang, Z., Liu, Y., Yang, S., Yang, N., Feng, C., Cai, Q., Evers, J.B., van der Werf, W., Zhang, L., 2018. Agroforestry enables high efficiency of light capture, photosynthesis and dry matter production in a semi-arid climate. Eur. J. Agron. 94, 1–11.

Zhang, Y., Li, X., Šimůnek, J., Shi, H., Chen, N., Hu, Q., 2022. Optimizing drip irrigation with alternate use of fresh and brackish waters by analyzing salt stress: The experimental and simulation approaches. Soil Tillage Res. 219, 105355.

Zhao, W., Zhou, Q., Tian, Z., Cui, Y., Liang, Y., Wang, H., 2020. Apply biochar to ameliorate soda saline-alkali land, improve soil function and increase corn nutrient availability in the Songnen Plain. Sci. Total Environ. 722, 137428.

Zong, R., Wang, Z., Zhang, J., Li, W., 2021. The response of photosynthetic capacity and yield of cotton to various mulching practices under drip irrigation in Northwest China. Agric. Water Manag. 249, 106814.